



## D2.7 – Report on mechanical properties of the coated interconnects (T2.4)

### PROJECT INFORMATION

GRANT AGREEMENT NUMBER	826323
PROJECT FULL TITLE	Low Cost Interconnects with highly improved Contact Strength for SOC Applications
PROJECT ACRONYM	LOWCOST-IC
FUNDING SCHEME	FCH-JU2
START DATE OF THE PROJECT	1/1-2019
DURATION	36 months
CALL IDENTIFIER	H2020-JTI-FCH-2018-1
PROJECT WEBSITE	<a href="http://www.lowcost-ic.eu">www.lowcost-ic.eu</a>

### DELIVERABLE INFORMATION

WP NO.	2
WP LEADER	Ragnar Kiebach
CONTRIBUTING PARTNERS	DTU
NATURE	Report
AUTHORS	Peyman Khajavi, Yousef Alizad Farzin, Henrik Lund Frandsen
CONTRIBUTORS	Ragnar Kiebach
CONTRACTUAL DEADLINE	01/06/2020
DELIVERY DATE TO EC	24/08/2020 – draft version

### DISSEMINATION LEVEL

PU	Public	X
PP	Restricted to other programme participants (incl. Commission Services)	
RE	Restricted to a group specified by the consortium (incl. Commission Services)	
CO	Confidential, only for the members of the consortium (incl. Commission Services)	

## 1 Introduction

In Solid Oxide Fuel and Electrolysis Cell (SOCs) technologies, interconnects are used to connect single cells in the stacks. The interconnects should be chemically and mechanically durable under the typical operating condition/cycling of SOCs. Crofer 22 H and APU are widely used but rather expensive interconnects materials. Efforts on developing cheaper, yet durable interconnects would be highly advantageous for the development of SOCs technologies. The ferritic stainless steel 411 coated with a thin CoCe layer is reported as a cost-effective alternative to other common interconnects materials such as Crofer. The CoCe coating layer can mitigate the issue observed in uncoated 411, i.e. increasing area specific resistance (ASR) caused by e.g. formation of insulating silica scales [1–3].

In this study, we evaluate the mechanical adherence of the CoCe-coating on the AISI 411 steel at 750 and 850 °C. For this, a glass-ceramic sealant with high fracture energy (i.e. 23.7 J/m<sup>2</sup>, [4]) is joined to coated steel bars in a sandwiched structure (see **Fig. 1**). When broken apart, the intent is to have the coating pulled off the steel substrate because of the strong adherence to the glass. The robust glass-ceramic sealant applied in this work thus acts as a “glue” between the top and bottom steel bars. The robustness of the coated layer and crack propagation path are investigated using four-point and fractography analyses is used to ensure that the fracture occurs in the coating/steel interface.

Due to problems with sub-supplier and consequent movement of our labs and the Corona pandemic, we have not been able to age the samples for 3000 hours, only 250 hours, and the current version is thus a draft of the final version, once our labs are operational.

## 2 Experimental

The experimental procedure carried out in this study is schematically shown in **Fig. 1**.

### 2.1 Screen printing ink and substrates

The glass-ceramic sealant powder (referred to as V11 sealant) was prepared using the method described in [4,5]. Table 1 presents the chemical composition of the V11 sealant [5]. The precursor materials were mixed, fired at 1350 °C for 2 h, and then quenched in water. The resulting glass was then ball-milled using a planetary ball mill. The screen-printing ink was prepared using a mixture of the V11 sealant powder, Dipropylene Glycol (DPG, solvent), and Polyvinylpyrrolidone (PVP) K30 (dispersant) and K90 (binder).

The CoCe coated ferritic stainless 411 steel was provided by Sandvik Materials, a product marketed as Sandvik Sanergy<sup>®</sup> HT 441. The as-received metallic sheets were laser cut to two sets of rectangular samples (bars), i.e. having the size of 29 × 3 mm<sup>2</sup> and 60 × 3 mm<sup>2</sup> (**Fig. 1**).

### 2.2 Sample preparation

The prepared ink was screen printed onto one side of the small bars. One big bar was then placed on the top of two screen-printed samples in a sandwiched structure (**Fig. 1**). The applied symmetric

structure creates a 2 mm wide notch on the bottom of the samples. The sandwiched samples were then fired at 800°C while using a load of 16.7 N/cm<sup>2</sup>.

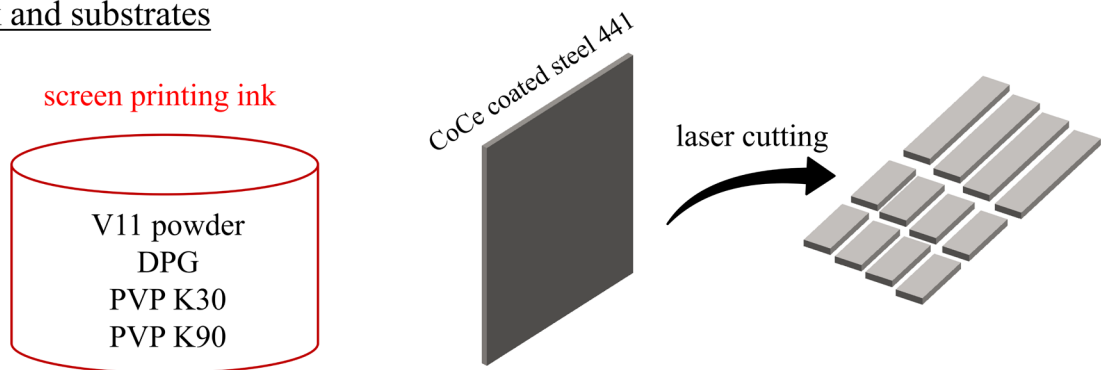
The sintered samples were aged at 750 and 850 °C for 250 h in air and used for mechanical and fractography analyses.

### **2.3 Mechanical testing and fractography**

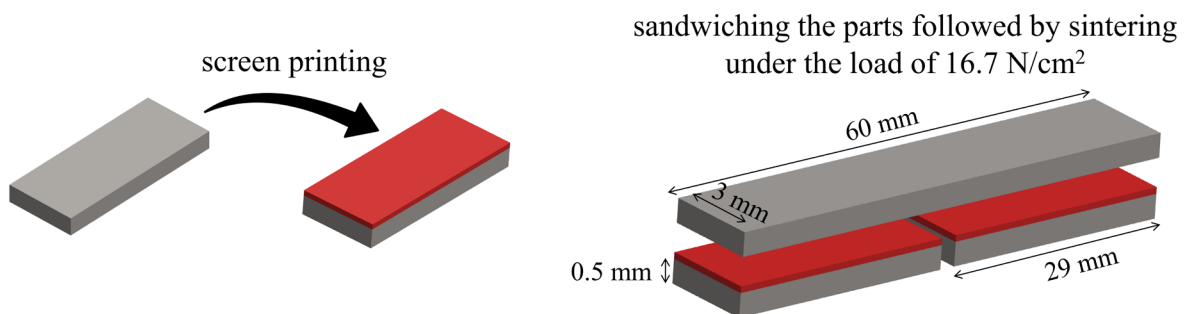
The aged samples were tested using four-point bending. The loading configuration in the four-point bending tests is schematically shown in **Fig. 1, III**. The tests were conducted at room temperature using a loading rate of 0.6 mm/min. A detailed description of the load-displacement curves and the analysis is described elsewhere [4].

After the mechanical measurements, the post-mortem analysis on the fractured samples was conducted using Scanning Electron Microscopy (SEM) and Energy Dispersive X-ray spectroscopy (EDX).

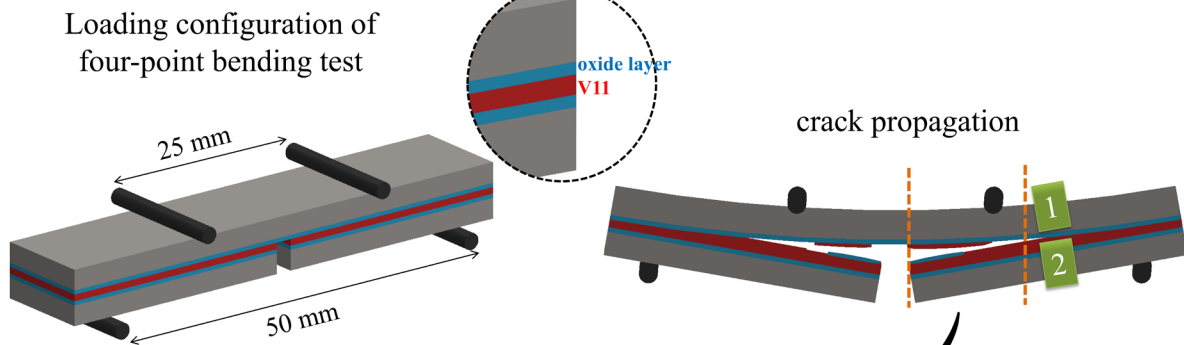
### I. Ink and substrates



### II. Sample preparation



### III. Mechanical testing



### IV. Fractography

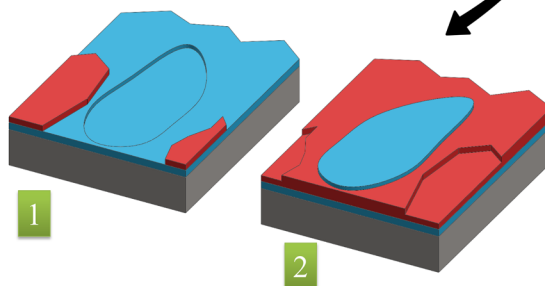


**Figure 1** Experimental procedure in the present study: I. screen printing ink and substrates, II. sample preparation (screen printing and sintering), III. four-point bending test and IV. SEM and EDX analysis of the fractured surfaces. The blue and red colors show schematically the oxide layer formed during aging, and the screen-printed V11 glass-ceramic layer, respectively.

### 3 Results and discussion

**Fig. 2** shows the room temperature fracture energy of the sandwiched samples after 250 h of aging at 750 and 850 °C. The inherent fracture energy of the V11 glass, as reported in [4] is also presented in the figure. As seen, the fracture energy of the sandwiched samples increased by increasing the aging temperature.

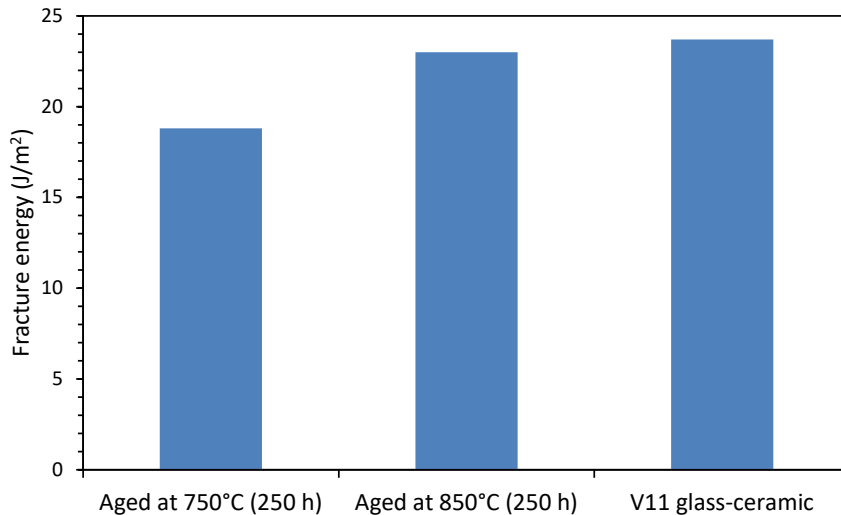


**Figure 2** Fracture energy measured at room temperature for glass-ceramic sandwiched coated steel 411 samples after aging at 750 and 850°C for 250 h in air, and the inherent fracture energy of the used glass-ceramic reported in [4].

SEM micrograph and EDX analysis of the top fractured surface (the long bar, i.e. section **1** in **Fig.1 III**) are presented in **Fig. 3**. Elemental analysis shows the presence of Si near the two edges of the fractured surface, while Mn and Cr are found between the Si rich areas. It is hence clear that the crack has propagated partly through the glass layer, and partly through the oxide layer/substrate interface of the CoCe-coated 441 substrate. This has schematically been shown in **Fig. 1, III and IV**.

From **Fig. 2**, the fracture energy of the sandwiched samples is comparable to the inherent fracture energy of the V11 sealant. Accordingly, and since the crack has propagated through the oxide and glass layers (as found by the elemental analysis), the fracture energy of the CoCe-coated 441 steel interconnects interface is concluded to be comparable to that of the V11 glass, i.e. 20-23 J/m<sup>2</sup>.

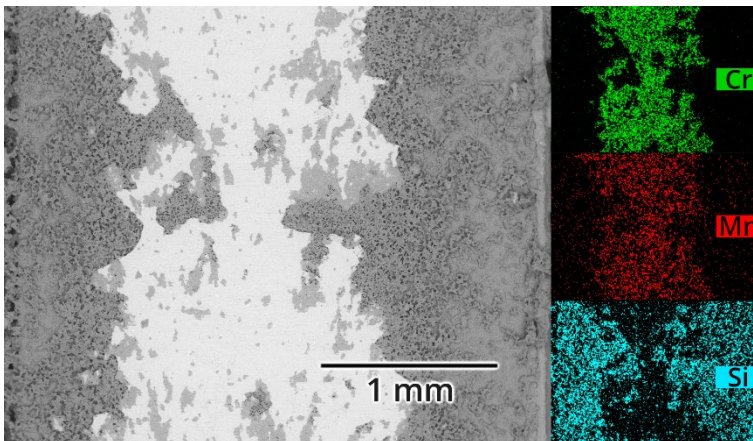


**Figure 3 SEM micrograph and elemental analysis of the fractured surface of the top (long) bar after the four-point bending test.**

## 4 Conclusions

The measured fracture energy is well above the values reported for preoxidized Crofer 22 APU (15.9 J/m<sup>2</sup>) and MnCo<sub>2</sub>O<sub>4</sub>-coated Crofer 22 APU (13.6 J/m<sup>2</sup>); and comparable to that of Alumina-coated Crofer 22 APU (23.7 J/m<sup>2</sup>) [4].

The adherence of the coating of on the steel of the cost-effective Sandvik Sanergy® HT 441 interconnects solution is hence concluded comparable to other state-of-the-art interconnect / coating solutions.

## Acknowledgment



This project has received funding from the Fuel Cells and Hydrogen 2 Joint Undertaking under grant agreement No 826323. This Joint Undertaking receives support from the European Union's Horizon 2020 research and innovation programme, Hydrogen Europe and Hydrogen Europe research.

## References

- [1] B. Talic, I. Ritucci, R. Kiebach, P.V. Hendriksen, H.L. Frandsen, Improved Robustness and Low Area Specific Resistance with Novel Contact Layers for the Solid Oxide Cell Air Electrode, *ECS Trans.* 91 (2019) 2225–2232.
- [2] J.G. Grolig, J. Froitzheim, J.E. Svensson, Coated stainless steel 441 as interconnect material for solid oxide fuel cells: Evolution of electrical properties, *J. Power Sources.* 284 (2015) 321–327.
- [3] Z. Yang, G.G. Xia, C.M. Wang, Z. Nie, J. Templeton, J.W. Stevenson, P. Singh, Investigation of iron-chromium-niobium-titanium ferritic stainless steel for solid oxide fuel cell interconnect applications, *J. Power Sources.* 183 (2008) 660–667.
- [4] I. Ritucci, R. Kiebach, B. Talic, L. Han, P. Zielke, P. V. Hendriksen, H.L. Frandsen, Improving the interface adherence at sealings in solid oxide cell stacks, *J. Mater. Res.* 34 (2019) 1167–1178.
- [5] I. Ritucci, K. Agersted, P. Zielke, A.C. Wulff, P. Khajavi, F. Smeacetto, A.G. Sabato, R. Kiebach, A Ba-free sealing glass with a high coefficient of thermal expansion and excellent interface stability optimized for SOFC/SOEC stack applications, *Int. J. Appl. Ceram. Technol.* 15 (2018) 1011–1022.